

NASA Technical Memorandum 89077

INTERDISCIPLINARY AND MULTILEVEL OPTIMUM DESIGN

Jaroslav Sobieszczanski-Sobieski and
Raphael T. Haftka

December 1986

(NASA-TM-89077) INTERDISCIPLINARY AND
MULTILEVEL OPTIMUM DESIGN (NASA) 49 p

CSCL 01C

N87-15205

G3/05 40395
Unclas



National Aeronautics and
Space Administration

Langley Research Center
Hampton, Virginia 23665

INTERDISCIPLINARY AND MULTILEVEL OPTIMUM DESIGN

Jaroslav Sobieszczanski-Sobieski
NASA Langley Research Center
Hampton, Virginia 23665 USA

and

Raphael T. Haftka
Virginia Polytechnic Institute and State University
Blacksburg, Virginia 24061 USA

INTRODUCTION

Engineering system design used to be compartmentalized by discipline. Material specialists would design better materials, fluid mechanics specialists would design optimum shapes, structural analysts would produce optimum structural designs based on materials and loads obtained by material and fluid mechanics specialists, and so on. Occasionally, interdisciplinary effects forced cooperation between disciplines. Aeroelastic phenomena such as flutter or loss of control-surface effectiveness forced aerodynamic and structural analysts to cooperate in the creation of the new discipline of aeroelasticity. However, when such interdisciplinary phenomena did not force cooperation, very little existed, beyond the conceptual design level.

While integrated design is more truly optimal than compartmentalized design (e.g., ref. 1), the difference in performance was not enough of an incentive to overcome the difficulties associated with design integration until two modern developments provided an additional incentive to do so.

The first development is the advent of tailored materials such as graphite-epoxy composites which permit the designer to tailor material properties to suit the specific requirements of the system being designed. The second development is the introduction of active control systems which permit a designer to improve performance through the use of a control system rather than by improving structural, aerodynamic, acoustic or other system characteristics.

The increasing interdisciplinary nature of the design process is most noticeable in the aerospace industry. A case

in point is the Grumman X-29A forward-swept-wing fighter for which composite materials were tailored to produce favorable aerodynamic-structure interaction. Because a metal swept-forward wing has an inherently destabilizing interaction between bending and twisting, it is not practical to build this type of wing with metal. However, a composite material was developed to reverse this destabilizing interaction and make the X-29A design feasible.

Integration in the design of complex engineering systems can be achieved at the governing equations level, by decomposition into self-contained but coupled tasks, or by judicious use of both approaches.

Equation-level integration in analysis typically begins with a realization that a number of disciplines contribute terms to equations that describe a particular physical phenomenon. Then, it is logical to form a unified set of equations from the terms contributed by the participating disciplines, research the best ways of solving these equations, and build operational experience by verification tests and applications.

In most cases equation-level integration is not required to describe physical phenomena, and integration is useful only for obtaining superior designs. Then integration by decomposition is in order. Each discipline remains a self-contained task. The integration is achieved by defining the interdisciplinary information channels, and finding the best ways of sequencing (iterating) the disciplinary computations. The sequencing can be strictly serial, figure 1, or it can exploit parallelism that leads to a hierarchial arrangement shown in figure 2. Frequently, a mix of the serial and parallel schemes is appropriate.

The same two approaches may be distinguished with regard to synthesis. Equation-level synthesis relies on equation-level integrated analysis in the same manner as single discipline synthesis - as a source of data describing the behavior and sensitivity of the object being optimized. The optimization procedure is shown in figure 3.

The same scheme can accommodate synthesis based on analysis decomposed serially by placing the content of figure 1 in the "ANALYSIS" box in figure 3. Examples of this type of multidisciplinary optimization applied to a large space-based antenna structure and a glider configuration are provided later.

However, if the analysis is decomposable in a way shown in figure 2, then the optimization can also be decomposed as shown in references 2, 3, giving rise to a multilevel optimization scheme illustrated in figure 4. According to reference 4, each box in the scheme can represent a physically separable subsystem (object decomposition), or a discipline analyzing one of many aspects of the same object (aspect decomposition).

The scheme relies on the separate optimization subtasks self-contained within subsystems or disciplines, and on sensitivity derivatives of the optimum to the inputs coming from the next higher level in the decomposition hierarchy. An example of one such sensitivity derivative is a derivative of minimum structural weight with respect to the wing aspect ratio. An algorithm for computing optimum sensitivity derivatives without engaging in a costly finite difference procedure is given in reference 5. Optimization of the entire system uses these derivatives for approximate assessment of the effects of system-level design decisions on the subsystems and contributing disciplines.

The objective of the present paper is to survey multidisciplinary optimization applications and focus on multilevel optimization as a means for integrating the design process. The paper begins with a survey of multidisciplinary optimization problems, continues by reviewing one practical multilevel optimization technique applied to a generic system and concludes with an example of a multilevel multidisciplinary optimization.

SURVEY OF INTERDISCIPLINARY OPTIMIZATION PROBLEMS

In some distant future we may expect that engineering system design will be fully integrated. At the present, design integration is typically proceeding by combining the

design process of two or three disciplines. The following survey discusses briefly several areas of multidisciplinary optimization and then describes in more detail two multidisciplinary design studies.

Controls and Structures

Active control systems are intended to reduce the demands on the structure by load alleviation or by active damping. Load alleviation systems anticipate naturally occurring loads and add loads that tend to cancel some of these original loads. A typical example is the load alleviation system designed for the B-52 Bomber which senses gusts ahead, and deflects control surfaces to alleviate them. Similar systems (called active suspension) are envisioned for future cars which will sense the bumpiness of the road and apply compensating loads to improve ride quality.

Active suspension systems also include an active damping component in that they sense vibrations and apply forces to damp them out. This active vibration damping is particularly important in applications to large and flexible space structures (e.g., ref. 6).

At present the control and structure design are compartmentalized with the control system designer assuming that the structural design is given. There is, however, a growing interest in simultaneous control/structure design (see ref. 6 for additional references). As shown in reference 6, the compartmentalized design approach can result in very large weight penalties if it leads to a structure which is too flexible.

Material and Structure

Tailored materials such as graphite-epoxy composites permit the designer to tailor material behavior to suit the structural application. For example, by proper selection of ply orientations it is possible to produce a composite laminate with a miniscule coefficient of thermal expansion, suitable for minimizing thermal deformations in large space antennas. Similarly, it is possible to take advantage of the different failure characteristics of various ply combinations. For example, reference 7 shows that the failure load of

compression-loaded plates with holes can be increased by removing the zero plies from a strip containing the hole.

At the present, while there is substantial interaction between composite material designers and structural designers, the design process is still disjoint. This is not acceptable because in composite materials, both material response and failure characteristics depend on the structural applications. That is, the same composite material can display vastly different characteristics when used in different structures. Therefore, optimum structural design must be coupled with the material design process to produce a true optimum, and to prevent unexpected failure modes.

Structures and Aerodynamics

The interaction between structures and aerodynamics is strong enough so that even in the traditional design process it was considered a separate superdiscipline - aeroelastic design. However, the aeroelastician worried only about aeroelastic interactions where the deformations of the structure affect the aerodynamic loads. Thus aeroelastic design considered phenomena such as divergence, flutter, and control surface effectiveness. Aeroelasticians did not consider the possibility of using the structural deformation to improve aerodynamic performance (because the effect is too small in metal aircraft), or changing the aerodynamic design to reduce structural weight. This latter trade-off between aerodynamic and structural performance was considered in an approximate way in the conceptual design stage.

With the growing use of composite materials designers are beginning to consider using structural deformations to improve aerodynamic performance. The next section of this paper contains an example of combined aerodynamic/structural design of a glider. It was performed by a cooperative effort between aerodynamicists and structural analysts, rather than by a person or a group who mastered both disciplines.

Structure and Heat Conduction

Currently there is little interaction between the thermal design and structural design of systems subjected to high thermal loads. A typical example is a reentry vehicle which

requires thermal protection systems such as insulation, ablation shields, or passive and active cooling systems. In the current design process the thermal protection system is designed to keep the temperature of the structure below a specified limit. The structure is then designed to carry the thermal and mechanical loads at that temperature. The current interaction between the two design processes is due to the fact that the structural material distribution affects the temperature distribution.

Reference 8 showed that the sequential thermal/structural design process is not always optimal. The combined design process can reduce the total weight of the system by overdesigning the thermal protection system to produce a structure operating at lower temperatures where its strength is higher. The combined design approach is facilitated by finite element software packages which permit the analyst to perform both the structural and thermal analysis simultaneously.

MULTIDISCIPLINARY DESIGN EXAMPLES

To complete this survey of interdisciplinary optimization problem, we consider in more detail two multidisciplinary design studies. The two have in common a serial decomposition approach (see fig.3).

Aerodynamic/Structural Optimization of Glider Wing

The integrated aerodynamic/structural design of the glider wing (ref. 9) is an example of combined optimization where the disciplinary analyses are performed separately and integrated through the optimizer. This case also provides an example of the pay-offs of integrated design.

The glider mission is to fly over a distance by gaining altitude circling in a thermal, and then glide to the next thermal, losing altitude in the process (see fig. 5). One measure of performance used in the study was the cross-country speed of the glider which is the average speed considering both phases of the flight. A second measure of performance was the weight of the glider for a given cross-country speed. The design variables and constraints are summarized in tables 1, 2 and figures 6, 7. Two optimization procedures used to

demonstrate the advantage of the integrated approach are shown schematically in figure 8. The first is a sequential approach, typical of the traditional compartmentalized approach. The aerodynamic design is first obtained for an initial estimate of the weight by varying the aerodynamic variables to maximize the cross country speed. The loads based on this aerodynamic design are then used to optimize the structure for minimum weight, and the new weight is used to restart the aerodynamic design. The process was considered converged when the change in weight from one iteration to the next was less than 0.2 percent. The combined optimization varies simultaneously both the aerodynamic and structural parameters to obtain the optimum design. The combined approach is able to take advantage of two interactions that the sequential approach cannot. The first interaction is the reduction in structural weight that can be achieved by modifications in aerodynamic shape, and the second is the improvement in aerodynamic performance which can be achieved by tailoring structural deformations.

The two design procedures were applied to a simple model of the wing. The aerodynamic analysis was based on lifting line theory, the aerodynamic design variables controlled the planform and twist distribution, and constraints were placed on maximum angle of attack and bank angle. The structural analysis was based on a beam model, the design variables were skin and web thickness and spar-cap areas, and constraints were placed on stresses and the divergence speed. The results of the two optimization procedures are compared in table 3. The iterated sequential design performance was only one percent inferior in the performance to the integrated design. However, this one percent in performance was parlayed into an 11 percent weight gain, when the combined design was optimized for minimum weight. The reason for the disparity is that the structural design was limited to orthotropic skin (no changes in ply orientations or percentages of various plies allowed) so that no anisotropic aeroelastic tailoring for improving aerodynamic performance was available. On the other hand,

there was complete freedom to tailor the aerodynamics to help the structure.

Optimization of Antenna Parabolic Dish Structure for Minimum Weight and Prescribed Emitted Signal Gain

This particular optimization application has been described in reference 10. The object of optimization is the minimum weight design of the support structure of a large (55 m diameter) parabolic dish antenna shown in figure 9. The support structure is made up of two surface lattices held apart by connecting struts forming a tetrahedral-cell truss. The concave side lattice is overlaid with a fine wire mesh that forms a parabolic reflector converting the electromagnetic radiation emitted from the feed placed in the focus into a coherent beam.

In orbit, the antenna moves through the Earth shadow and changes its orientation relative to the Sun. The resulting heating which varies over the structure and also in time distorts the support structure and the parabolic reflector surface causing a loss of emitted signal strength. The optimization calls for finding the cross-sectional areas of the support trusses such that the structural weight is minimum while not permitting the surface distortion to rise above the level that would weaken the electromagnetic radiation below a prescribed limit.

Two design variables were chosen to control three cross-sectional areas: one for all members in both of the two surface lattices, and one for all the connecting truss members. The analysis begins with thermal analysis to determine the member temperatures at a particular location on orbit. The temperatures are functions of the member cross-sections and generate stresses and deformations which are calculated next. The deformations are passed to the electromagnetic radiation analysis program to obtain the resulting weakening of the emitted signal.

Thus, the analyses are arranged serially as shown in figure 10 (the thermal and thermal-structural analyses were executed in this implementation as processors of the same finite element programming system, reference 11). Derivatives

required for optimization, performed by a useable-feasible directions algorithm (ref. 12), were obtained by a finite difference procedure. In keeping with the programming system approach (ref. 13), the optimizer was coupled directly not with the full analysis (boxes TA, SA, EMRA in fig. 10), but with an approximate analysis (box AA) to conserve the computer resources and to leave their control in the hands of the user. The approximate analysis is a linear, derivative-based extrapolation with an automatic switching to reciprocal variables as proposed in reference 14.

The results shown in figure 9 indicate a weight reduction by more than 1/3 from the initial value representing the best design achieved without systematic optimization. The surface precision as measured by the deflection RMS value has also improved, and the emitted signal strength measured by the gain value was kept above the required minimum of 19000. Judging by the results the optimizer reduced weight and distortion together. This occurred because in a thermally loaded structure, the internal forces may be reduced by reducing the structural sizes. The optimizer took advantage of this and achieved increased performance and reduced weight.

MULTILEVEL OPTIMIZATION

The last two examples, the glider and the antenna, demonstrated benefits attainable when optimization of engineering systems is carried out by means of stringing out disciplinary analyses in a sequence coupled to an optimizer set to improve a measure of system performance under all the appropriate constraints. The set of analyses included in the sequence responds to the optimizer requests for information as if it was a single analysis; therefore, one may call this arrangement optimization with integrated analysis.

Although this arrangement is demonstrably effective, it may not be practical for very large design tasks involving numerous engineering staff. Engineers tend to cluster into specialty groups operating concurrently. This time-honored mode of operation, which results in a broad work front reducing the design elapsed time, requires decomposition of the system optimization into several smaller sub-optimizations

each assigned to an engineering group. The remainder of the paper is devoted to an algorithm that supports such decomposition while preserving the internal couplings of the system optimization problem.

This section introduces multilevel optimization by decomposition in a particular formulation that applies to structures. As shown in reference 15, it is natural to base that formulation on the well-known analysis by substructuring which is a form of the object decomposition.

Optimization Terminology

An optimization formulation without decomposition serves as a reference from which the multilevel optimization algorithm is derived. The optimization is defined in terms of: the design variables, Z_b (see Table 4 for notation), which are the cross-sectional dimensions of the structural components; the objective function $F(Z)$ that can be any computable function of these variables (structural mass is the frequent choice); and the constraints, $g_w(Z)$ imposed on the behavior variables to account for the potential failure modes. Writing constraint functions as

$$g = d/c - 1 \leq 0 \quad (1)$$

the optimization problem in a standard formulation is

$$\min F(Z); \text{ such that } g_w(Z) \leq 0 \quad (2)$$

and requires a search of the design space considering all the design variables and constraints concurrently. In contrast, the algorithm presented in the next section breaks the problem into a number of search and analysis operations, each concerned with a smaller number of design variables and constraints.

Preliminary Definitions

The diagram in figure 11 shows a structure decomposed into several levels of substructures. The term "substructure" will refer to any entity in this decomposition scheme including the extremes of the full, assembled structure represented by the box on the top of the pyramid and single structural components representing the ultimate geometrical details appropriate to the problem at hand. The substructure levels are numbered from 1 on the top to i_{\max} at the bottom.

The hierarchical nature of the scheme instigates the use of the term "parent" to the structure at level i which, in turn, is decomposed into a number of "daughter" substructures at level $i+1$. A daughter may have only one parent and that parent must be at the level immediately above. Thus, it will be convenient to label each substructure SS_{ijk} , where i denotes the level, j defines the position at the level i counting from the left, and k identifies the parent's position at the level $i-1$. The substructure occupying the lowest position in a particular parent-daughter succession represents the ultimate level of detail at which the decomposition stops. There is no requirement that all such substructures must be at the same bottom level i_{\max} . In discussions involving more than one substructure, the triplets nlp , mkl , ijk , are used to distinguish among the substructures forming the hierarchy shown in figure 12.

Substructuring analysis (e.g., refs. 16, 17, 18) establishes the following functional relations (note that the subscript for the parent substructure is omitted):

$$Q^{ij} = f(K^{bij}, P^{bij}) \quad (3)$$

$$K^{bij} = f(K^{ij}) \quad (4)$$

$$K^{ij} = f(K^{bi+1,j}) = S_K(K^{bi+1,j}) \quad (5)$$

$$M^{ij} = f(M^{i+1,j}) = \sum_j M^{i+1,j} \quad (6)$$

$$P^{bij} = f(P^{ij}) \quad (7)$$

$$P^{ij} = S_P(P^{bi+1,j}) \quad (8)$$

The symbol f appearing in equations 3-8 denotes a general functional relationship which is different for each equation, and is computable in a manner prescribed by the particular substructuring algorithm chosen. For example, equations 4 and 7 take the form of matrix equations given in reference 17, Ch.9, Sec.1, as equations 9.13 and 9.14, respectively.

For SSijk at the ultimate level of detail, the distinctions between K^{bij} , p^{bij} , and K^{ij} , p^{ij} vanish, and K^{ij} , M^{ij} , derive directly from Z^{ij} . Consequently:

$$K^{bij} = K^{ij} \quad (9)$$

$$p^{bij} = p^{ij} \quad (10)$$

$$K^{ij} = f(Z^{ij}) \quad (11)$$

$$M^{ij} = f(Z^{ij}) \quad (12)$$

The local constraints that arise in SSijk at the ultimate level of detail involve calculation of stresses, strains, local buckling, etc., from Q^{ij} and Z^{ij} . In addition, constraints may be imposed on the internal forces, critical forces, and displacements of SSijk to account fully for all the constraints that would have been included in the one-level optimization problem represented by equation 2.

Although the foregoing definition of substructuring analysis is based on the finite element stiffness method, the use of a finite element analysis is not mandatory for the multilevel optimization algorithm presented here. As far as that algorithm is concerned, the analysis is a "black box" where only the inputs and outputs are important.

Multilevel Optimization Algorithm

With the substructuring scheme and analysis established in the foregoing, this section describes the optimization algorithm itself. The essentials of the computer implementation are also given.

Basic Concept.— The basic idea for the proposed multilevel optimization by substructuring stems from the elementary observation, based on equations 3 through 8, that the effect of a daughter SSijk on its parent SSi-1,kl is felt only through K^{bij} , M^{ij} , and p^{bij} which depend on $K^{b,i+1,j}$, $M^{i+1,j}$, and $p^{b,i+1,j}$, respectively. Consequently, the entries of $K^{b,i+1,j}$, $M^{i+1,j}$, and $p^{b,i+1,j}$ may be manipulated as generalized design variables without disturbing the results of the SSi-1,kl analysis as long as the entries of K^{bij} , M^{ij} , and

P^{bij} are held constant. If these entries are held constant, then the boundary forces Q^{ij} acting on every $SSijk$ in $SSi-1,kl$ remain constant and the effect of manipulating the generalized design variables in a particular $SSijk$ is limited to that $SSijk$ itself and its daughters. As explained later, the purpose of the above manipulation of the matrix entries is not to minimize the substructure mass M^{ij} which, as stated above, remains constant. Instead, the purpose is to improve satisfaction of the constraints in the $SSijk$ and its daughters, while performing the task of the total mass optimization at the assembled structure level.

Invariance of the entries K^{bij} , M^{ij} , and P^{bij} can be enforced by rewriting equations 4 through 8 as equality constraints.

$$h_K^{ij} = K^{bij} - f(K^{bi+1,j}) = 0 \quad (13)$$

$$h_M^{ij} = M^{ij} - f(M^{i+1,j}) = 0 \quad (14)$$

$$h_P^{ij} = P^{bij} - f(P^{bi+1,j}) = 0 \quad (15)$$

Equations 13, 14, and 15 establish the entries of K^{bij} , M^{ij} , and P^{bij} as given parameters in optimization of $SSijk$. Simple replacement of indices renders these equations valid for $SSi-1,kl$ and redefines the optimization parameters of the daughter $SSijk$ as generalized design variables in the optimization of its parent $SSi-1,kl$, so that

$$\{X^{i-1,k}\} = \{Y^{ij}\} \quad (16)$$

$$\{Y^{ij}\}^t = \{K^{bij} | M^{ij} | P^{bij}\}^t \quad (17)$$

These equations define a recursive relation of the variables and parameters that extends from the top of the substructuring scheme to the bottom.

Of course, the number of design variables T^{ij} must exceed the number of constraints V^{ij} (which is equal to the number of individual equations in the vector equations 13, 14, and 15).

$$T^{ij} > V^{ij} \quad (18)$$

for a design freedom to exist, allowing for the symmetry of the stiffness matrices. Otherwise, if

$$T^{ij} \leq V^{ij} \quad (19)$$

then the equality constraints of equations 13 through 15 either define the SSijk design variables uniquely or overdetermine them.

The basic concept outlined above translates into an algorithm to be introduced now in detail.

Optimization at the most detailed level.- Introduction of the optimization algorithm begins at the level of the most detailed substructures. Consequently, equations 9 through 12 apply and the design variables are the cross-sectional dimensions so that

$$x^{ij} = z^{ij} \quad (20)$$

and the parameters (held constant during optimization at this level) are

$$\{y^{ij}\}^t = \{K^{ij} | M^{ij} | P^{ij}\}^t \quad (21)$$

It is assumed that a complete, top-down, substructuring analysis for an initial structure has been carried out so that for an SSijk one has computed its Q^{ij} , while its M^{ij} , z^{ij} , K^{ij} , and P^{ij} are given.

Optimization for improvement of inequality constraint satisfaction is achieved by minimizing a single measure representing all the constraints and called the cumulative constraint, a concept similar to the use of a penalty function. A differentiable cumulative constraint function can be obtained (as it was in ref. 19) by means of the Kreisselmeier-Steinhauser function (KS) defined in reference 20.

$$C^{ij} = KS(g_w^{ij}) = 1/\rho \ln \left(\sum_w \exp(\rho g_w^{ij}) \right) \quad (22)$$

that has the property of approximating the maximum constraint so that

$$\max_w (g_w^{ij}) < KS(g_w^{ij}) < \max_w (g_w^{ij}) + 1/\rho \ln (W^{ij}) \quad (23)$$

with the factor ρ controlled by the user. Thus, the KS function serves as a convenient single measure of the degree of constraint violation (or satisfaction).

Analysis of SSijk yields the local inequality constraints as

$$g_w^{ij} = f(x^{ij}, y^{ij}, Q^{ij}) \quad (24)$$

Based on the above definitions, the optimization problem is formulated.

$$\min_{x^{ij}} C^{ij}(x^{ij}, y^{ij}, Q^{ij}) \text{ such that} \quad a) \quad (25)$$

$$h_K^{ij} = 0 \quad b1)$$

$$h_M^{ij} = 0 \quad b2)$$

$$h_P^{ij} = 0 \quad b3)$$

$$L^{ij} \leq x^{ij} \leq U^{ij} \quad c)$$

Solution of this optimization problem (by any technique available) yields a constrained optimum described by a vector π^{ij} composed of the minimum value of the cumulative constraint, \bar{C}^{ij} , and the optimal vector of the design-variables, \bar{x}^{ij}

$$\pi^{ij} = \{\bar{C}^{ij} | \bar{x}^{ij}\}^t \quad (26)$$

This solution depends on y^{ij} and Q^{ij} , and the derivatives $d\pi^{ij}/dy_z^{ij}$ may be expressed by a chain differentiation to account for equations 3 and 21 that tie Q^{ij} to y^{ij}

$$d\bar{C}^{ij}/dy_z^{ij} = \partial\bar{C}^{ij}/\partial y_z^{ij} + \sum_r (\partial\bar{C}^{ij}/\partial Q_r^{ij})(\partial Q_r^{ij}/\partial y_z^{ij}) \quad (27)$$

$$d\bar{x}^{ij}/dy_z^{ij} = \partial\bar{x}^{ij}/\partial y_z^{ij} + \sum_r (\partial\bar{x}^{ij}/\partial Q_r^{ij})(\partial Q_r^{ij}/\partial y_z^{ij}) \quad (28)$$

In equations 27 and 28, the partials of \bar{C}^{ij} with respect to y_z^{ij} and with respect to Q_r^{ij} are obtained from the algorithm described in reference 5, and the partial Q_r^{ij} with respect to y_z^{ij} by conventional structural sensitivity analysis. Parenthetically, one may add that the algorithm of reference 5 uses second derivatives of constraints that may be expensive to calculate. However, a modified version of the algorithm is available in reference 21 that avoids the cost of second derivatives and calculates the sensitivity derivatives for \bar{C}^{ij} , but not for \bar{x}^{ij} .

Optimization of the lowest parent substructure.- The design variables for all parent substructures control the stiffness and mass distribution in that substructure. They could be elements of the substructure boundary or mass matrices, or quantities which control these entries. Because these substructure design variables are not necessarily tangible quantities, they are referred to in the following as "generalized" design variables. As shown in figure 12, the parent substructure SS_{mk1} , $m=i-1$, receives from its daughters, SS_{ijk} , the minimized values of their cumulative constraints, \bar{C}^{ij} , optimal values of their design variables, \bar{X}^{ij} , and the optimum sensitivity derivatives of these quantities with respect to parameters, Q^{ij} and Y^{ij} , calculated from equations 27 and 28.

Preparing for the formulation of the optimization problem for the parent substructure, we consider the recursive relation between the design variables and parameters according to equations 16 and 17, and recognize that equations 9 through 12 do not apply. When optimizing the parent substructure, we want to improve satisfaction of the assembled substructure inequality constraints, such as limits on its elastic deformations and stability that depend on the substructure stiffness, mass, and boundary forces:

$$g^{mk} = g^{i-1,k} = f(X^{mk}, Y^{mk}, Q^{mk}) \quad (29)$$

At the same time, we want to improve constraint satisfaction in all the substructure daughters. These can be approximated (as in ref. 19) by linear extrapolation of their cumulative constraints using the derivatives from equation 27 and replacing Y^{ij} with X^{mk} according to equation 16.

$$\bar{C}_e^{ij} = \bar{C}_o^{ij} + \sum_t (d\bar{C}^{ij}/dX_t^{mk}) \Delta X_t^{mk} \quad (30)$$

This extrapolation plays a key role in the algorithm because it approximates the daughter-parent coupling without incurring the expense of reoptimizing the daughters (repeating eq. 25) for every change of the parent design variables.

Including the \bar{C}_e^{ij} values together with g^{mk} in a cumulative constraint formed by the KS function we have

$$C^{mk} = 1/\rho \ln \left(\sum_w \exp(\rho g_w^{mk}) + \sum_j \exp(\rho \bar{C}_e^{ij}) \right) \quad (31)$$

and the optimization problem to be solved for the parent SSi-1,k1 is

$$\min_{X^{mk}} C^{mk}(X^{mk}, Y^{mk}, Q^{mk}) \text{ STOC} \quad a) \quad (32)$$

$$h^{mkt} = \{h_K^{mk} | h_M^{mk} | h_P^{mk}\}^t = 0 \quad b)$$

$$L^{mk} \leq X^{mk} \leq U^{mk} \quad c)$$

$$L^{ij} \leq X_e^{ij} \leq U^{ij} \quad d)$$

where

$$X_e^{ij} = X_o^{ij} + \sum_t (d\bar{X}^{ij}/dX_t^{mk}) \Delta X_t^{mk} \quad (33)$$

The increment ΔX^{mk} is defined as

$$\Delta X^{mk} = X^{mk} - X_o^m \quad (34)$$

The constraints of equation 32b are analogous to equations 25b1, b2, b3 written in a compact format. The constraints of equation 32c incorporate the side constraints to prevent the design variables from attaining physically impossible values (e.g., negative diagonal entries in a stiffness matrix) and include the move limits to control the extrapolation errors introduced by equation 30. The constraints of equation 32d are introduced to keep the design variables in the daughters from exceeding their side constraints. These constraints are not essential because their function may be performed directly by the daughter side constraints. In fact, omitting the constraints of equation 32d eliminates the need for the derivatives of \bar{X}^{ij} and allows replacing the algorithm of reference 5 by the much less costly algorithm of reference 21. However, these constraints are included in this description for completeness.

Solution of the problem of equation 32 generates the result vector and its derivatives that are analogous to those of equations 26, 27, and 28 with the indices ij replaced by m=i-1, and k.

Optimization of the next parent structure. - Moving on to the substructure SSnlp, everything stated in the preceding

subsection on optimization of SSmkl applies to SSnlp directly, provided that: the indexes n , l , and p are replaced by another triplet, say, α , β , γ , that identifies the parent of SSnlp at the level $\alpha = n-1$; and the indexes m , k , l are replaced by n , l , p . For consistency, equation 32d, if used, should be replicated to encompass fully each line of succession emanating downward from SSnlp. Beyond these changes, no new conceptual elements are introduced, and no additional definitions or discussion are needed at the junctions between the levels until one arrives at the top level. Hence, any number of intermediate levels of substructuring can be inserted, if physically justified, into a line of succession extending downward from the assembled structure on the top; i.e., the algorithm is recursive.

Optimization of the assembled structure.— The assembled structure is designated SS110. Its optimization problem is similar to the one described for a parent substructure SSmkl with the following differences:

1. No parameters are defined solely for the decomposition purposes; therefore, there is no need for the equality constraints to enforce constancy of the mass and the boundary stiffnesses.
2. The objective function is the mass of the assembled structure.
3. There is no need for a single cumulative constraint (unless one needs it to reduce the number of constraints to be processed at that level).
4. The boundary forces are the external loads on the assembled structure.

Accounting for these differences, the optimization problem for the top level is

$$\min_{11} M^{11} (X^{11}) \text{ such that}$$

$$X^{11} \quad \text{a) (35)}$$

$$g^{11} \leq 0 \quad \text{b)}$$

$$\bar{c}_e^{2j} \leq 0 \quad \text{c)}$$

$$L^{11} \leq X^{11} \leq U^{11} \quad \text{d)}$$

$$L^{2j} \leq \bar{X}_e^{2j} \leq U^{2j} \quad e)$$

where equation 35e is analogous to equation 32d with the limits L^{2j} , U^{2j} applied in conjunction with extrapolations of the type expressed by equation 33, extended recursively to encompass all the levels below as mentioned in the subsection on SSnlp. Unlike in the daughters SSijk, the optimization of SS110 does not have to be analysed for the optimum sensitivity. Information transmitted to the top level optimization problem is indicated in figure 12.

Iterative procedure.- When the SS110 optimization is completed, the entire structure has acquired a new distribution of stiffness and mass within the move limits. Hence, the analysis must be repeated and followed by a new round of substructure optimizations in an iterative manner until convergence. Accordingly, the procedure follows these steps:

1. Initialize all cross-sectional dimensions.
2. Perform a substructuring analysis, including for each substructure at each level the transformation of the stiffness matrix into the boundary stiffness matrix and the transformation of the forces applied to the interior degrees of freedom to the forces coinciding with the boundary degrees of freedom. Calculations of the behavior derivatives needed for the ensuing optimizations and for the optimum sensitivity analyses are included in the substructuring analysis.
3. Perform the operations of optimization and optimum sensitivity analysis as defined by equations 25 through 34.
4. Optimize the assembled structure as defined by equation 35.
5. Repeat from step 2 and terminate only when: all constraints g^{ij} are satisfied at all levels and M^{11} has entered a phase of diminishing returns.

This procedure is illustrated in figure 13 by a flow chart in the Chapin's chart format (ref. 22).

Salient features of the algorithm.- In perspective, the multilevel algorithm differs from a single-level one in a number of the following salient features.

A multitude of smaller problems, that may be processed concurrently, replace a single large problem. Although the subproblems are isolated, their coupling is preserved because the influence of the changes in the parent on the daughters is represented by linear extrapolation based on the optimum sensitivity and behavior sensitivity derivatives. With the exception of the most detailed level, the stiffness and mass distributions are controlled directly by generalized design variables. Mass is the objective at the top level, while the constraint satisfaction improvement is the objective at all levels below.

Selection of the generalized design variables is a matter of judgment. In the extreme case, one may choose to control as design variables all entries of the boundary stiffness matrix, boundary forces vector, and mass of each daughter; although, intuitively, this would seem impractical. Experience will probably show that a limited control, e.g., over the diagonal entries of the stiffness matrix only, will suffice in most cases.

The overall procedure building blocks; i.e., the operations of substructure analysis, constraint calculations, optimization, and the behavior and optimum sensitivity analyses are "black boxes" whose algorithmic contents may be freely replaced provided that the input/output definitions remain unchanged. For example, different types of structural analysis may be used at each level and even for each substructure, as it will be shown in the numerical example.

PORTAL FRAME EXAMPLE

Problem Description.- The subject algorithm was tested by optimizing, with and without decomposition, a framework structure similar to the one used in references 19, 23, and 24. As shown in figures 14 and 15, the framework assembled at level 1 decomposes into three box beams, each beam being a substructure at level 2. Finally, each beam decomposes into three walls (the fourth wall is symmetric), each wall being

the most detailed substructure at level 3. The external loads were applied at one corner of the framework as shown in figure 14. There were no interior loads on the substructures.

The objective was to minimize the structural material volume subject to constraints on the displacements of the loaded point, the in- and out-of-plane elastic stability of each beam treated as a column, and the stresses and local buckling of the wall panels treated as stringer-reinforced plates. There were also minimum gage constraints and the physical realizability constraints on the cross-sectional dimensions.

The objective functions, design variables, parameters, and constraints are defined for the multilevel optimization in table 5. A comprehensive description of all the physical and computational details of the test problem is given in reference 15.

Tools for Analysis and Design Space Search.- A finite element analysis was used to calculate the framework's displacements and the beam end-forces. Stresses in the beams loaded with the end-forces were computed by engineering beam theory. The beams were treated as columns for stability analysis, and local buckling of the walls was based on closed form "designer handbook" formulas provided in references 25, 26, and implemented as described in reference 27.

At each level, the optimization was conducted by the same general-purpose nonlinear mathematical programming code CONMIN, based on the useable-feasible directions technique and documented in reference 28.

Three-Level Optimization.- The framework was first optimized without decomposition to establish reference results. Then, the multilevel optimization algorithm was applied to the structure decomposed as shown in figures 14 and 15. In the decomposition, the stiffened panels are daughters clustered in triplets under a parent box beam. The beams, in turn, are daughters of the assembled structure.

As shown in table 5, the top level optimization manipulates the beam extensional and bending stiffnesses through the cross-sectional areas and bending moments of

inertia. The cross-sectional area also controls the beam volume which contributes directly to the objective function.

At the middle level, the stiffnesses expressed by the area and moment of inertia become fixed parameters and the variables are the wall membrane stiffnesses controlled by the geometrical dimension variables. These variables, and consequently the membrane stiffnesses become fixed parameters at the bottom level at which the ultimate detail dimensions are engaged as variables. The equality constraints arise between the parameters and variables. Owing to relative simplicity of the expressions involved, (see Appendix, ref. 15), these constraints were solved explicitly.

Examination of table 5 in conjunction with the previous description of the analysis tools illustrates the point that dissimilar analyses may be used as needed at different places in a decomposition scheme.

The sensitivity analysis of behavior was carried out by a single step forward finite difference technique. The optimum sensitivity analysis was based on the algorithm given in reference 5.

Results and Remarks on the Method Performance.- Figure 16 shows a sample of results obtained with and without decomposition. The starting points for both methods are the same. The normalized plots illustrate the objective function, a selected individual constraint, and a cumulative constraint containing the above individual constraint as they varied over the iterations. An iteration is defined in the optimization without decomposition as the following set of operations: one analysis including gradients, computation of a useable-feasible search direction, and finding a constrained minimum in that direction. In the three-level optimization, it is defined as one execution of the series of steps listed in the procedure definition in the previous section.

The results verified that the multilevel algorithm was capable of finding a feasible design having an objective function close to and, in some cases lower than, the reference optimization without decomposition. As in reference 19, differences up to 72.1% were observed among the detailed

design variables obtained by the two methods. However, these differences were no larger than those observed by comparing the designs obtained without decomposition starting from different initial design points. Therefore, these differences can be attributed to the problem non-convexity. The jagged appearance of the graphs in figure 16 is a characteristic of the usable-feasible directions search algorithm, amplified in the multilevel optimization by the extrapolation errors. A detailed comparison of the results from both methods is given in reference 15.

Regarding computational efficiency, the main intrinsic advantage of the multilevel algorithm is in its capability to process the subproblems concurrently. Demonstration of this advantage would require a large application, distributed computing, and division of work among many people. Consequently, computational efficiency was not one of the goals in execution of the relatively small numerical example on a conventional serial computer. However, the example showed that the amount of computational labor per iteration was less in the multilevel algorithm than in the single-level, conventional one, and that both algorithms required about the same number of iterations for convergence. The example also showed that for the multilevel algorithm programming of the operations of data moving and bookkeeping was the dominant effort.

DECOMPOSITION APPROACH IN OPTIMIZATION OF A GENERIC ENGINEERING SYSTEM

In the preceding discussion, the multilevel optimization by decomposition was introduced using a structure that was partitioned into components - an example of an object decomposition. This section describes that approach as it was extended in reference 3 to a case of a generic engineering system decomposable in both the object and aspect sense.

Decomposition of Two-Level System.- The key to the proposed approach is a formalized decomposition of the large design problem into a set of smaller manageable subproblems coupled by means of the sensitivity data that measure the change of the subsystem design due to a change in the system design.

Let ES be an engineering system composed of the subsystems $SS_1, \dots, SS_2, \dots, SS_i, SS_n$ as shown in figure 17 (the abbreviations are defined in table 6, and table 7 gives examples for the generic quantities in the context of aircraft design). The design variables are grouped in a vector SV for ES and the vectors DV_i for SS_i . The ES has a performance index PS that should be maximized within the system constraints collected in a vector GS. The ES imposes demands on each SS_i . These demands are quantified by entries of a vector DS_i which depends on SV through analysis of ES. Each SS_i is designed by manipulating DV_i so that it meets its DS_i , regarded as constants, while maximizing its safety margin SM_i representing (e.g., by using the KS function, ref. 20) a set of subsystem constraints GSS_i . These tasks, separate for each SS_i , can be carried out concurrently by whatever means the SS_i designers choose, including the appropriate analysis, optimization, and also judgment and experimentation.

A new element required under the proposed approach is evaluation of the sensitivity of the maximum (optimum) SM_i to changes in DS_i in the form of optimum sensitivity derivatives $\partial SM_i / \partial DS_i$. At the ES level, these derivatives combined with the derivatives $\partial DS_i / \partial SV$ in chain differentiation yield the sensitivity of SM_i to changes in SV in the form of derivatives $\partial SM_i / \partial SV$. The maximum SM_i and its derivatives show the ES designer, with a linear extrapolation accuracy, how the change of SV that he controls will affect the SM_i for each SS_i . Guided by this information and by the ES analysis, the ES designer can decide which variables in SV to change and by how much in order to move toward the goal of satisfying all the constraints GS and GSS_i while maximizing the PS. The SV change will alter the DS_i . Responding to that, the SS_i designers modify their designs and pass updated information to the ES designer who, then, changes the SV again, and so on. In this manner, the ES and the SS_i designers carry on a systematic iteration toward an improved system design, trading data in the form of DS_i , SM_i , and their derivatives. Each designer works on a separate assignment with the control of PS vested in the ES designer, while the SS_i designers focus on

their SS_i feasibility. The whole problem is decomposed, yet remains coupled by the ES- SS_i data exchange shown in figure 17.

Overall Procedure. - Based on the above qualitative description, one may now formulate a step-by-step procedure to implement the decomposition approach.

Step 1. Initialize the system.

Step 2. Analyze the system. Calculate PS, GS, DS_i , and $\partial DS_i / \partial SV$.

Step 3. Design subsystems SS_i . The DV_i are manipulated within upper and lower bounds, L_i and U_i , so as to maximize SM_i for given DS_i . The latter requires vector of equality constraints GE_i for those DS_i that are also functions of DV_i . These constraints enforce equality of the DS_i values prescribed at the system level and computed as a function of DV_i so that

$GE_i = DS_i(SV) - DS_i(DV_i) = 0$. Formally, the task may be formulated as an optimization problem

$$\begin{aligned} \max_{DV_i} SM_i(DV_i, DS_i) \quad & \text{subject to constraints} \quad (36) \\ GE_i(DV_i, DS_i) &= 0 \end{aligned}$$

$$L_i \leq DV_i \leq U_i$$

The output of the operation is: $\overline{SM}_i = (SM_i)_{\max}$, and the optimal subsystem design variables, \overline{DV}_i .

Step 4. Analyze each SS_i design for sensitivity to the inputs received from the system to obtain the $\partial SM_i / \partial DS_i$.

Step 5. Modify the SV to improve the system design. In this operation, one uses the $\partial DS_i / \partial SV$, \overline{SM}_i , and $\partial \overline{SM}_i / \partial DS_i$ obtained in Steps 2, 3, and 4, to extrapolate each SM_i as a function of the increment ΔSV

$$SM_i(\Delta SV) = \overline{SM}_i + \frac{\partial \overline{SM}_i}{\partial DS_i} \frac{\partial DS_i}{\partial SV} \Delta SV \quad (37)$$

Improvement of the system design may be formalized as an optimization:

$$a) \max_{SV} PS(SV) \text{ subject to constraints} \quad (38)$$

$$b) GS(SV) \leq 0, \quad c) \overline{SM}_i(SV) \geq 0 \text{ (for all } i)$$

$$d) L \leq SV \leq U$$

in which the system level analysis provides the PS and GS, and the \overline{SM}_i in equation 38c is approximated by equation 37. The bounds in equation 38d include "move limits" protecting the accuracy of the extrapolation in equation 38c. The above optimization problem may have no feasible solution within the move limits in equation 38d if it begins with significant constraint violations in equations 38b and c. If a feasible solution cannot be found, an acceptable outcome of equation 38 is a new design point moved as close to the constraint boundary as possible. The result of this step is a new SV defining a modified design of the system.

Step 6. Repeat from Step 2 until all the constraints GS are satisfied, all safety margins SM_i are non-negative, and the performance index PS has converged.

In the above procedure, also shown in figure 18, the analyses in Step 1 and 2 are problem-dependent. The behavior sensitivity analysis required to obtain the $\partial DS_i / \partial SV$ can be obtained by either a finite difference technique or, preferably, by a quasi-analytical method (e.g., ref. 29). The optimization defined by equations 36 and 38 can be carried out by any suitable algorithm. The extension of the above two-level algorithm to multilevel systems is given in ref. 2, and its application to aerospace systems is discussed in reference 30.

MULTILEVEL OPTIMIZATION STUDY OF A TRANSPORT AIRCRAFT

The general algorithm introduced in the preceding section has been tested in a design optimization study of a transport aircraft reported in reference 31. The procedure was applied to an existing transport aircraft, and the fuel for a particular mission was selected as the objective function. Everything in the aircraft system was fixed as in the existing

design, except for the airfoil depth-to-chord ratio, h , and the cross-sectional dimensions of the stringer-stiffened wing cover panels. Constraints included those typical for the aircraft performance requirements; e.g., runway length, climb rate, cruising speed, etc., and the strength and local buckling limits on stresses in the wing box covers.

The optimization was predicated on the trade-off between the structural wing weight and the drag, both being functions of " h ." In order to intensify that trade-off to obtain conclusive study results, the cruise Mach number was set at .90, significantly greater than in the subject aircraft. That artificially high Mach number made the wave drag a larger fraction of the total drag. The problem was a natural candidate for decomposition approach because it contained a very large number of detailed design variables (6 per each of 216 panels for a total of 1296 variables) which were distinct from the system-level configuration variable " h ." The analyses involved also differed in their nature, and ranged from a semi-empirical performance aerodynamics for entire aircraft, through a highly detailed finite element analysis of the wing box, to a handbook level stress and buckling analysis of each stiffened panel.

Following the approach described in the previous section, the problem was decomposed as shown in figure 19, and an iterative procedure was implemented, with each iteration consisting of top-down analyses and bottom-up optimizations. The existing aircraft data initialized the procedure.

The top, system-level analysis was carried out by a performance analysis program, reference 32, that included a semi-empirical aerodynamic analysis. The middle-level subsystem - the wing box - was analyzed by a finite element program, reference 11, and the resulting edge forces were applied to individual panels at the bottom level.

Optimizations began at the bottom level, separately for each panel. The objective function was the panel cumulative constraint representing all the stress and buckling constraints by means of the KS function, reference 20. The constraints included side constraints and equality constraints

on panel skin thickness and equivalent, smeared stringer thickness which preserved the thicknesses set at the wing box level. These equality constraints assured that the panel membrane stiffnesses stayed constant; hence, the edge forces remained constant, and the panel was isolated from its neighbors for the duration of its optimization. Sensitivity analysis was performed on each optimized panel using algorithms described in reference 5 to obtain derivatives of the minimized cumulative constraint with respect to the thicknesses and edge forces that were defined above as the optimization parameters.

The middle level optimization designed the skin thickness and the equivalent, smeared stringer thickness. Spanwise distributions of these thicknesses were described by polynomial functions whose coefficients were the design variables. The objective function was a cumulative constraint formed from the cumulative constraints that were minimized for each panel. At the middle-level, these constraints were extrapolated linearly using the optimum sensitivity derivatives with respect to the wing box thickness variables. The equality constraint on the wing box weight kept it constant at the value set at the top, system level. Optimum sensitivity derivatives were computed for the objective function with respect to "h" and the wing-box weight.

Finally, the optimization at the highest level used only two design variables: the depth-to-chord ratio, "h," and the wing box structural weight. Its objective function was the mission block fuel, and the inequality constraints included, in addition to the performance constraints, the wing box cumulative constraint that was minimized at the middle level. The latter constraint was extrapolated with respect to the design variables using the optimum sensitivity derivatives calculated at the middle level.

Nonlinear mathematical programming was used for optimization at all levels. The bottom and middle levels employed the usable-feasible directions algorithm. It was coupled directly to the analysis program at the bottom level, but at the middle level, it was coupled to an approximate

analysis (derivative-based extrapolation). A SUMT procedure incorporating the Davidon-Fletcher-Powell algorithm was implemented at the top level.

The study demonstrated that the procedure converged well, in 4 to 5 cycles, to the same end result when started from different initial design points (including the existing design). As seen in a sample of the optimization history, shown in figure 20, the convergence was reasonably smooth. Some improvements of both the fuel consumption and the wing-box structural weight were achieved relative to the existing design. The improvement of the fuel consumption was small, as expected when starting the optimization with an already refined design. Also, it has to be emphasized that the improvement should not be interpreted as an indication of the actual potential still remaining in the subject aircraft because the analysis was not as complete as the one that was used in support of the actual design (e.g., the gust loads were not considered, and manufacturing constraints were excluded). However, the study demonstrated a multilevel, multidisciplinary optimization system in operation.

CONCLUDING REMARKS

Modern developments such as the increasing use of composite materials tend to increase the interactions between various disciplines in the design of engineering systems. Interdisciplinary design approach will yield, in general, a better design, but requires a systematic algorithm to account for the interactions and to ensure convergence and efficiency. The paper presents a survey of some of the more important interdisciplinary interactions and examples of the benefits of interdisciplinary design. It then reviews multilevel optimization as a tool of breaking down the multidisciplinary design problem to a set of manageable tasks. A specific multilevel algorithm is first presented in the context of structural optimization and then generalized to engineering system design.

REFERENCES

1. Sobieszczanski-Sobieski, J.; Barthelemy, J. F.; and Giles, G. L.: Aerospace Engineering Design by Systematic Decomposition and Multilevel Optimization; International Council of Aeronautical Science, 14th Congress, Paper No. ICAS-84-4.7.3, 1984.
2. Sobieszczanski-Sobieski, J.: A Linear Decomposition Method for Large Optimization Problems. NASA TM-83248, 1982.
3. Sobieszczanski-Sobieski, J.; and Barthelemy, J-F.: Improving Engineering System Design by Formal Decomposition, Sensitivity Analysis and Optimization. Proceedings of International Conference of Engineering Design, Hamburg, West Germany, 1985. (R. Hubka, Editor), Vol. 1, pp. 314-321. Publisher: Heurista, Zurich.
4. Archer, B.: The Implication for the Study of the Design Methods of Recent Developments in Neighboring Disciplines. Proceedings of International Conference of Engineering Design, *ibid*, 161, pp. 833-840.
5. Sobieszczanski-Sobieski, J.; Barthelemy, J-F.; and Riley, K. M.: Sensitivity of Optimum Solutions to Problem Parameters. AIAA Journal, Vol. 20, 1982, pp. 1291-1299.
6. Haftka, R. T.: Optimum Control of Structures. Previous lecture, ASI.
7. Haftka, R. T.; and Starnes, J. H., Jr.: Use of Optimum Stiffness Tailoring to Improve the Compressive Strength of Composite Plates with Holes. AIAA/ASME/ASCE/AHS 26th Structures, Structural Dynamics and Materials Conference, Orlando, FL, April 1985.
8. Adelman, H. M.: Preliminary Design Procedure for Insulated Structures Subject to Transient Heating. NASA TP-1534, 1979.
9. Grossman, B.; Strauch, G.; Epperd, W. M.; Gurdal, Z.; and Haftka, R. T.: Integrated Aerodynamic/Structural Design of a Sailplane Wing. AIAA Paper No. 86-2623. AIAA Aircraft Systems Design and Technology Meeting, Dayton, OH, October 1986.
10. Adelman, H. M.; and Padula, S. L.: Integrated Thermal Structural Electromagnetic Design Optimization of Large Space Antenna Reflectors. NASA TM-87713, 1986.
11. Whetstone, W. D.: EISI-EAL: Engineering Analysis Language. Proceedings of the Second Conference on Computing in Civil Engineering, ASCE, 1980, pp. 276-285.

12. Vanderplaats, G. N.: The Computer Design and Optimization. Computing in Applied Mechanics (R. F. Hartung, Editor), AMD, Vol. 18, American Society of Mechanical Engineering, 1976; pp. 25-48.
13. Sobieszczanski-Sobieski, J.: From a Black Box to a Programming System. Chapter 11, Foundations of Structural Optimization: A Unified Approach. Edited by A. J. Morris, J. Wiley & Sons, New York, 1982.
14. Starnes, J. H., Jr.; and Haftka, R. T.: Preliminary Design of Composite Wings for Buckling, Stress, and Displacement Constraints. Journal of Aircraft, Vol. 16, 1979, pp. 564-570.
15. Sobieszczanski-Sobieski, J.; James, B. B.; and Riley, M. F.: Structural Optimization by Generalized Multilevel Optimization. AIAA Paper No. 85-0698. Proceedings of AIAA/ASME/ASCE/AHS 26th Structures, Structural Dynamics and Materials Conference, Orlando, FL, April 15-17, 1985. Also published as NASA TM-87605, October 1985.
16. Noor, Ahmed K.; Kamel, Hussein, A.; and Fulton, Robert E.: Substructuring Techniques--Status and Projections. Computers & Structures, Vol. 8, No. 5, May 1978, pp. 621-632.
17. Przemieniecki, J. S.: Theory of Matrix Structural Analysis. Chapter 9, McGraw-Hill Book Co., 1968.
18. Aaraldsen, P. O.: The Application of the Superelement Method in Analysis and Design of Ship Structures and Machinery Components. Presented at the National Symposium on Computerized Structural Analysis and Design, George Washington University, Washington, DC, March 27-29, 1972.
19. Sobieszczanski-Sobieski, J.; James, B.; and Dovi, A.: Structural Optimization by Multilevel Decomposition. AIAA Journal, Vol. 23, No. 11, 1985, pp. 1775-1782.
20. Kreisselmeier, G.; and Steinhauser, G.: Systematic Control Design by Optimizing a Vector Performance Index. Proceedings of IEAC Symposium on Computer Aided Design of Control Systems, Zurich, Switzerland, 1971.
21. Barthelemy, J.-F. M.; and Sobieszczanski-Sobieski, J.: Optimum Sensitivity Derivatives of Objective Function in Nonlinear Programming. AIAA Journal, Vol. 21, No. 6, 1983, pp. 913-915.
22. Chapin, Ned: New Format for Flowcharts. Software - Practice and Experience, Vol. 4, 1974, pp. 341-357.
23. Lust, R. V.; and Schmit, L. A.: Alternative Approximation Concepts for Space Frame Synthesis. AIAA Paper No. 85-0696-CP. AIAA/ASME/ASCE/AHS 26th Structures, Structural

Dynamics and Materials Conference, Orlando, FL, April 15-17, 1985.

24. Haftka, R. T.: An Improved Computational Approach for Multilevel Optimum Design. Journal of Structural Mechanics, 12(2), 1984, pp. 245-261.
25. Angermayer, K.: Structural Aluminum Design. Reynolds Metals Company, Richmond, VA, 1965.
26. Timoshenko, S. P.; and Gere, J. M.: Theory of Elastic Stability. McGraw-Hill, New York, 1961.
27. Sobieszczanski-Sobieski, J.: An Integrated Computer Procedure for Sizing Composite Air Frame Structures. NASA TP-1300, Hampton, VA, Feb. 1979.
28. Vanderplaats, G. N.: CONMIN--A FORTRAN Program for Constrained Function Minimization: User's Manual. NASA TM X-62282, August 1973.
29. Adelman, H. M.; and Haftka, R. T.: Sensitivity Analysis of Discrete Structural Systems. AIAA Journal, Vol. 24, No. 5, May 1986, pp. 823- 832.
30. Sobieszczanski-Sobieski, J.; Barthelemy, J. F.; and Giles, G. L.: Aerospace Engineering Design by Systematic Decomposition and Multilevel Optimization. International Council of Aeronautical Science, 14th Congress, Paper No. ICAS-84-4.7.3, September 1984.
31. Wrenn, G. A.; and Dovi, A. R.: Multilevel/Multidisciplinary Optimization Scheme for Aircraft Wing. NASA CR-178077, 1986.
32. McCullers, L. A.: Aircraft Configuration Optimization Including Optimized Flight Profiles. Proceedings of Symposium on Recent Experiences in Multidisciplinary Analysis and Optimization. NASA CP- 2327, Part 1, 1984, pp. 395-412.

Table 1: Design Variables for Glider Design

3 Performance Design Variables	1. Angle of attack at the root during the turn. 2. Angle of attack at the root during cruise. 3. Radius of the turn.
6 Geometric Design Variables	4. Angle of twist at the break relative to the root. 5. Angle of twist at the tip relative to the root. 6. Chord length at the root. 7. Chord length at the break. 8. Chord length at the tip. 9. Distance to the break.
24 Structural Design Variables	10-17. Spar cap thickness for each wing section. 18-25. Spar web thickness for each wing section 26-33. Skin thickness for each wing section.

Table 2: Design Constraints for Glider Wing

3	Stall Constraints during turning maneuver.	1. No stall at the root.
		2. No stall at the break.
		3. No stall at the tip.
3	Performance Constraints	4. Bank angle less than 50%.
		5. Climb speed greater than zero.
		6. Minimum divergence speed.
24	Structural Constraints (at 43 m/sec, 5.9 g)	7-14. Maximum spar cap strain for each wing section, .3%.
		15-22. Maximum shear stress for each wing section, web shear $\leq 6000 \text{ N/mm}^2$.
		23-30. Wing skin must satisfy Tsai-Hill strength constraint for each wing section.

Minimum average cross-country speed was also used as a constraint for weight minimized designs.

Table 3: Optimal Glider Designs

Iterated Sequential		Integrated Design	
		Maximum Cross-country Speed	Minimum Mass
Cross-country speed (m/s)	3.44	3.48	3.44
Mass of one wing (kg)	13.0	12.5	11.6

Table 4: Nomenclature for Multilevel Structural Optimization Algorithm

Quantities

A	Cross-sectional area.
C	Cumulative constraint (equation 22).
c	Capacity: limitation on the ability to meet a particular demand d (e.g., allowable stress).
d	Demand: a physical quantity the structure is required to have, to support, or to be subjected to in order to perform its function (e.g., stress).
F	Objective function.
$f()$	Functional relation.
g^{ij}	Vector of constraint functions, g_w^{ij} ; $w = 1 \rightarrow W^{ij}$.
h^{ij}	Vector of partitions h_K^{ij} , h_M^{ij} , h_P^{ij} (eq. 25b).
h_K^{ij} , h_M^{ij} , h_P^{ij}	Vectors of the equality constraints defined by equations 13, 14, and 15, respectively. The vector elements are, respectively: h_{KS1}^{ij} , h_{MS2}^{ij} , h_{PS3}^{ij} , where $S1 = 1 \rightarrow S_1^{ij}$, $S2 = 1 \rightarrow S_2^{ij}$, $S3 = 1 \rightarrow S_3^{ij}$.
I	Cross-sectional moment of inertia.
K^{ij}	Stiffness matrix of SSijk.
K^{bij}	Boundary stiffness matrix for SSijk.
L^{ij}	Lower bound on X^{ij} including move limits.
M^{ij}	Mass of SSijk (a scalar).
P^{ij}	Vector of the External loads applied to interior and/or boundary of SSijk.
Q^{ik}	Boundary forces, Q_r^{ij} , of SSijk, $r = 1 \rightarrow R^{ij}$.
P^{bij}	Vector of P^{ij} transferred to the boundary of SSijk:
Q^{ij}	Vector of the forces, Q_r^{ij} , $r = 1 \rightarrow R^{ij}$, acting on the boundary of SSijk.
Q^{ik}	Boundary forces, Q_r^{ij} , of SSijk, $r = 1 \rightarrow R^{ij}$.

S_K	Summation of stiffnesses contributed by substructures SS_{ijk} assembled in a parent substructure SS_{mkl} .
S_P	Summation of the boundary loads contributed by substructures, SS_{ijk} , assembled in a parent substructure SS_{mkl} .
SS_{ijk}	A substructure (including the extremes of the assembled structure and a single structural element).
SS_{mkl}	A substructure-parent of SS_{ijk} , $m = i-1$, see fig. 12.
SSS_{nlp}	A substructure-parent of SS_{mkl} , $n = m-1$, see fig. 12.
STOC	Acronym: <u>subject to constraints</u> .
T^{ij}	Total number of design variables for SS_{ijk} .
W^{ij}	Number of inequality constraints.
U^{ij}	Upper bound on X^{ik} including move limits.
V^{ij}	Number of constraints defined by eqs. (13)-(15).
X^{ij}	Vector of design variables, X_t , in SS_{ijk} , $t = 1 \rightarrow T^{ij}$.
Y^{ij}	Vector of the entries in K^{bij} , M^{ij} , and the entries in P^{bij} that are held constant as parameters in optimization of SS_{ijk} . The vector Y^{ij} contains V^{ij} elements Y_v^{ij} .
Z^{ij}	Vector of cross-sectional dimensions, Z_b^{ij} , $b = 1 \rightarrow B^{ij}$, used as design variables in SS_{ijk} that corresponds to a single structural element.
π	A vector defined by equation 26.
ρ	A user-controlled constant in the KS function (eq. 22).
Δ	Increment of a variable (see definition of subscript o)

Indices, Subscripts, and Superscripts Not Included in the Definitions Above

Overbar Denotes an optimal quantity

- b Superscript to denote an association with the SS boundary
- e Subscript to identify an extrapolated value
- o Subscript to identify an original (reference) value from which an increment is measured.

Table 5: Quantities Defined for the Multilevel Test Case Optimization

<u>TOP LEVEL</u>	
OBJECTIVE:	The framework material volume.
DESIGN VARIABLES:	A and I of the beams.
CONSTRAINTS:	Displacements of the loaded corner and C_e for the beams.
<u>MIDDLE LEVEL</u>	
OBJECTIVE:	Cumulative constraint C representing the column buckling and C_e for the walls.
DESIGN VARIABLES:	Wall membrane stiffness contributing to the beam axial and bending stiffnesses controlled through the dimensions shown in Fig. 14, Section A-A.
CONSTRAINTS:	Equality - beam cross-sectional area and moment of inertia.
<u>BOTTOM LEVEL</u>	
OBJECTIVE:	Cumulative constraint C representing a set of stress and local buckling constraints of the wall.
DESIGN VARIABLES:	Cross-sectional dimensions shown in Fig. 14, DETAIL B.
CONSTRAINTS:	Inequality - minimum gages, geometrical proportions, and geometrical realizability. Equality - membrane stiffnesses for tension-compression and bending of the wall in its own plane.

Table 6: Notation for Multilevel Generic Optimization

DS_i	vector of demand quantities imposed by the system on subsystem i .
DV_i	vector of design variables for subsystem i .
ES	(engineering) system.
GE_i	vector of equality constraints for subsystem i .
GS	vector of system inequality constraints; an inequality constraint is defined as $g = k(\text{DEMAND}/\text{CAPACITY}) - 1$, satisfied when $g \leq 0$.
GSS_i	vector of inequality constraints for subsystem i .
L, L_i	vector of lower limits on SV, and DV_i , respectively (move limits included).
PS	performance index for ES (a scalar).
SM_i	safety margin for SS_i (a scalar), defined as $SM_i = \max (\text{CAPACITY}/\text{DEMAND}) - 1$.
SS_i	subsystem i .
SV	vector of system design variables.
U, U_i	vector of upper limits on SV, and DV, respectively (move limits included).

Table 7: Examples of the Equivalents of the Generic Terms
Typical for an
Aircraft Application

DS_1	at the middle level: lift required of the wing; at the bottom level: edge loads N_x , N_y , N_{xy} on a wing cover panel.
DV_1	at the middle level: wing bending stiffness distribution; at the bottom level: detailed wing panel dimensions.
ES	aircraft, top (system) level.
GE_1	at the middle level: wing structure weight prescribed at the top level; at the bottom level: panel spanwise membrane stiffness prescribed at the middle level.
GS	runway length.
GSS_1	at the middle level: wing tip deflection; at the bottom level: panel local buckling.
PS	fuel economy for a given mission.
SS_1	the wing box, middle level; the wing cover stiffened panels, third (bottom) level.
SV	wing structural weight and airfoil thickness to chord ratio.
$\partial DS_1 / \partial SV$	derivative of wing lift with respect to structural weight.
$\partial SM_1 / \partial DS_1$	derivative of wing panel safety margin with respect to edge loads.

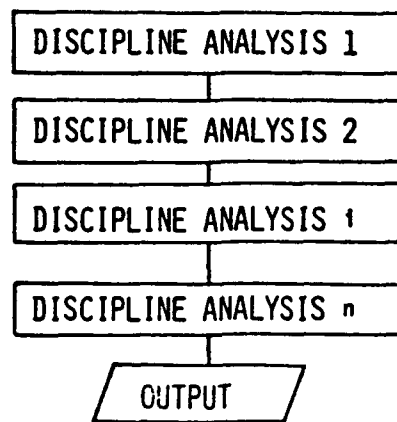


Figure 1. Many disciplinary analyses performed in series.

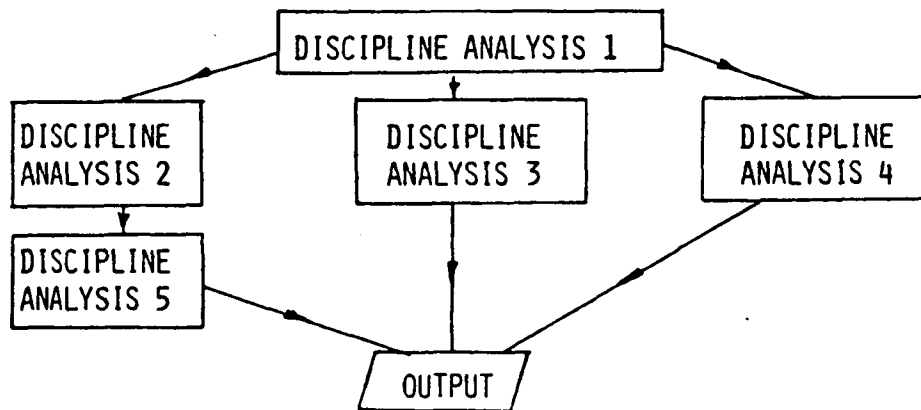


Figure 2. Disciplinary analyses in a hierarchical framework.

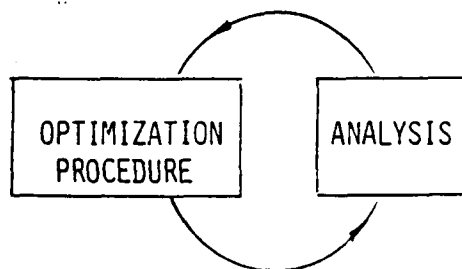


Figure 3. Multidisciplinary analysis coupled to an optimization procedure.

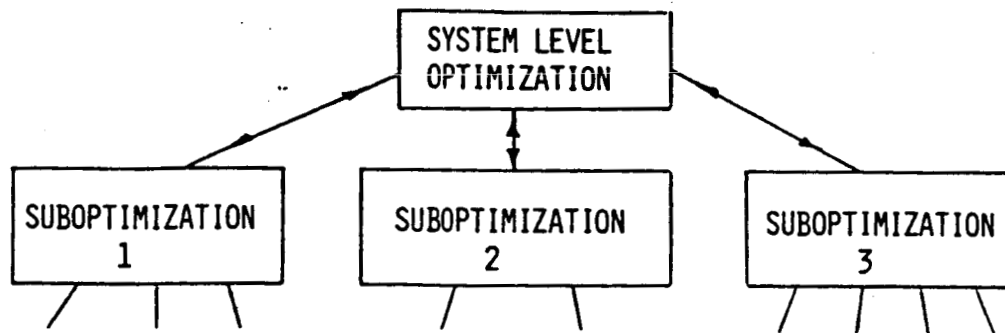


Figure 4. Multidisciplinary optimization as a hierarchy of subtasks.

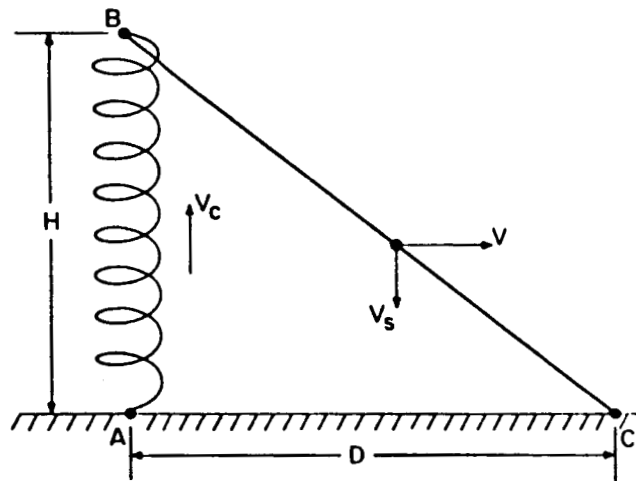


Figure 5. Glider mission profile.

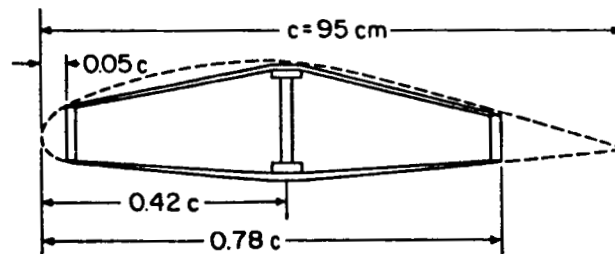


Figure 6. Typical cross-section of glider wing element.

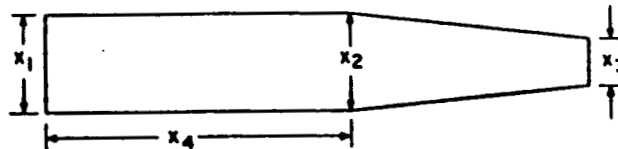


Figure 7. Planform geometry variables.

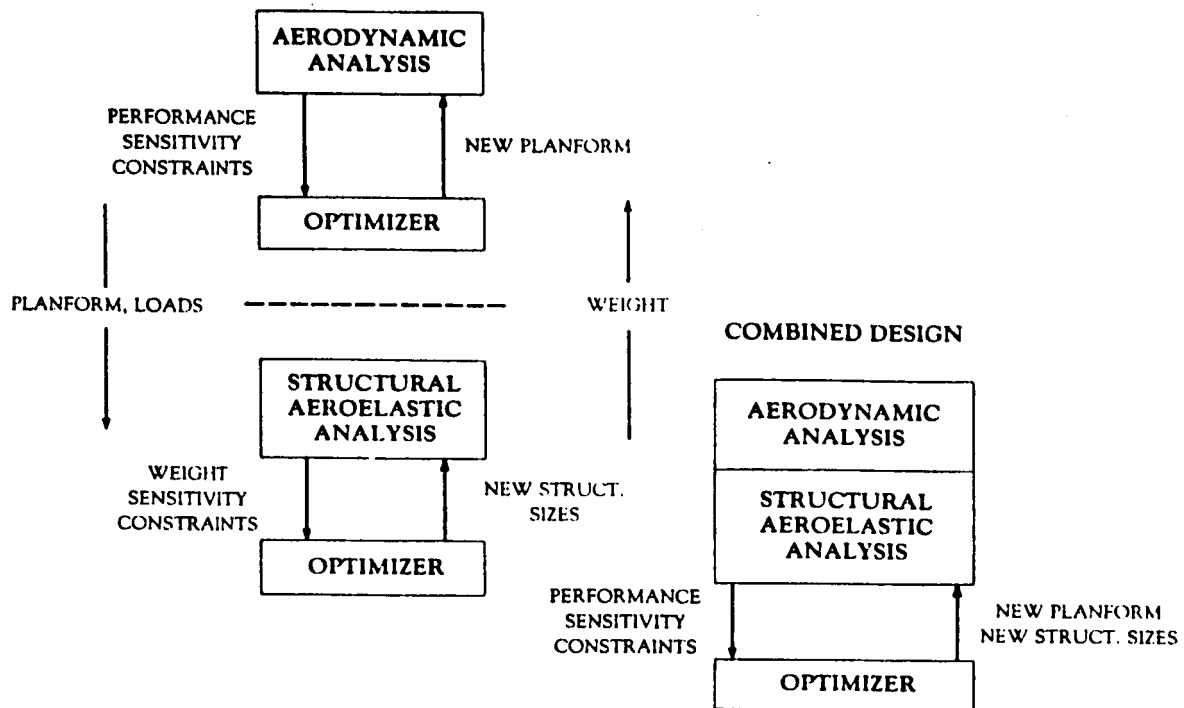


Figure 8. Schematic of sequential and integrated (combined) optimization procedures for glider wing.

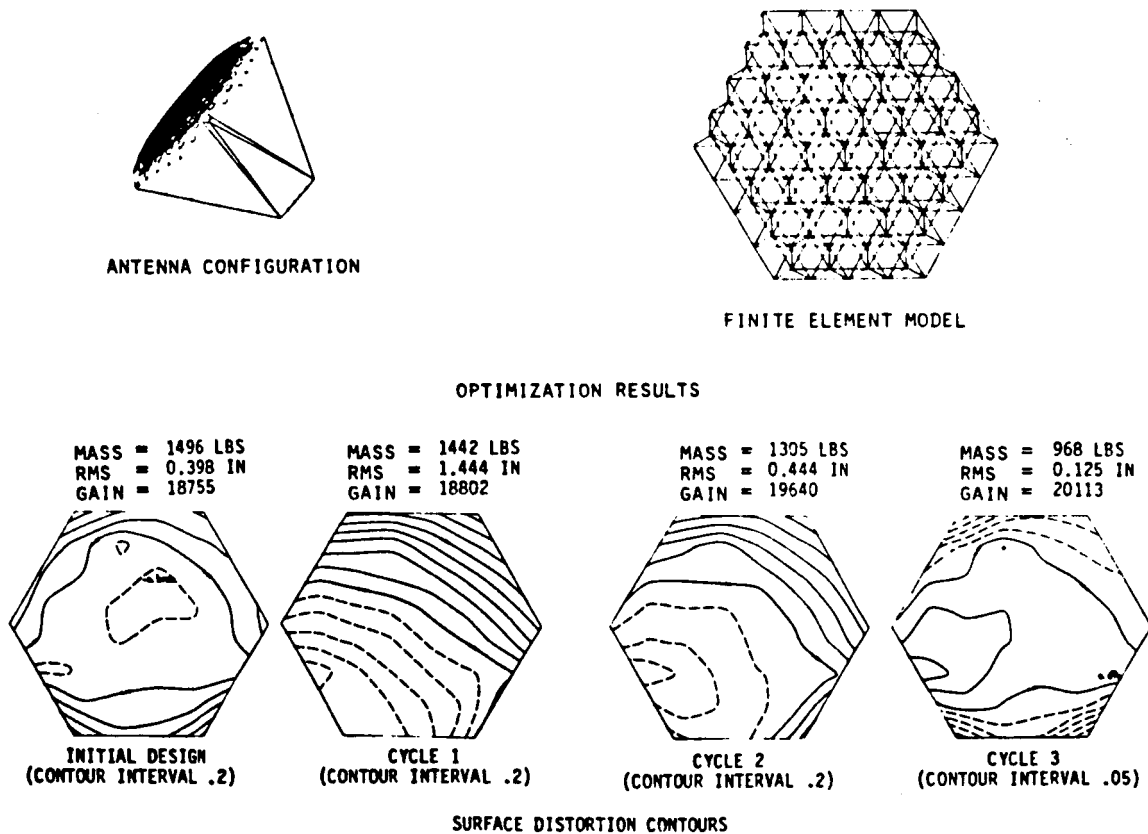


Figure 9. Antenna structure and optimization results.

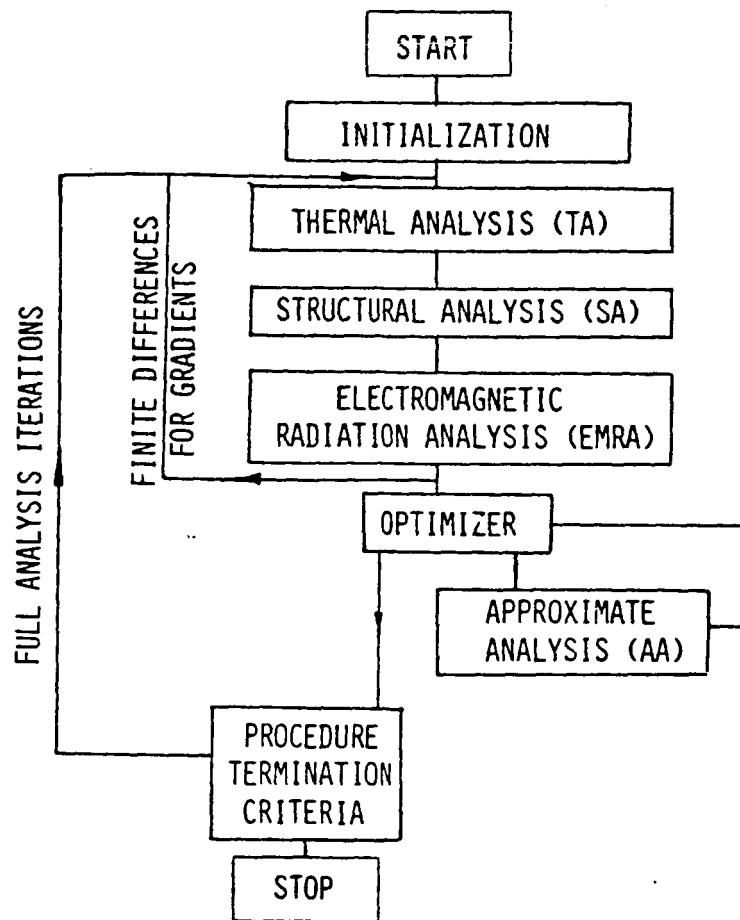


Figure 10. Antenna optimization procedure.

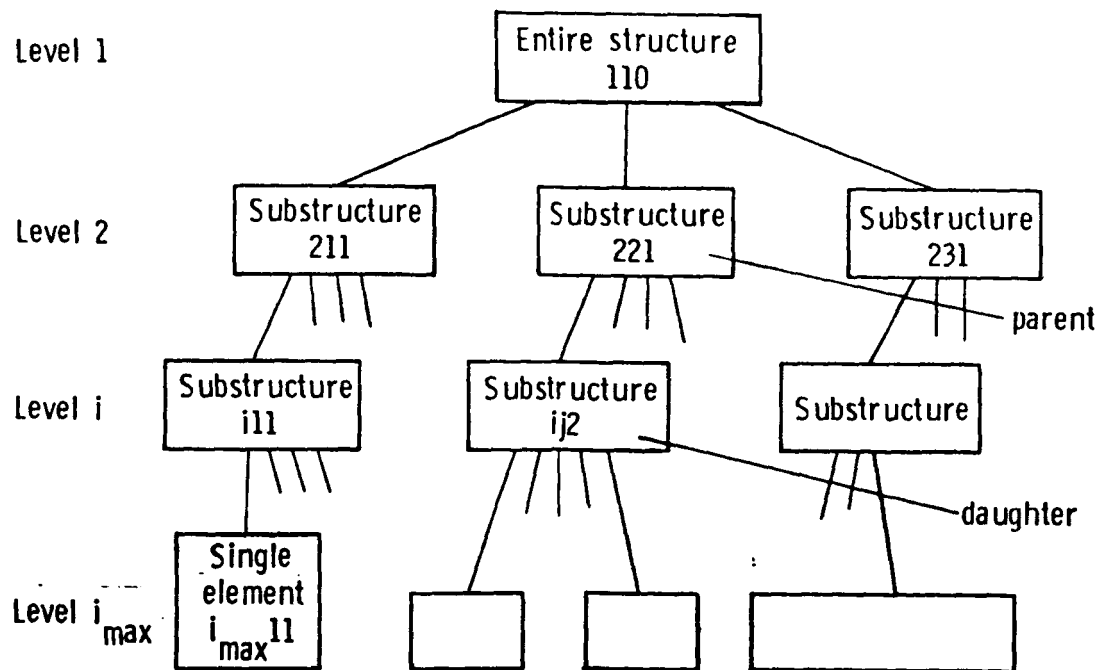


Figure 11. Multilevel substructuring.

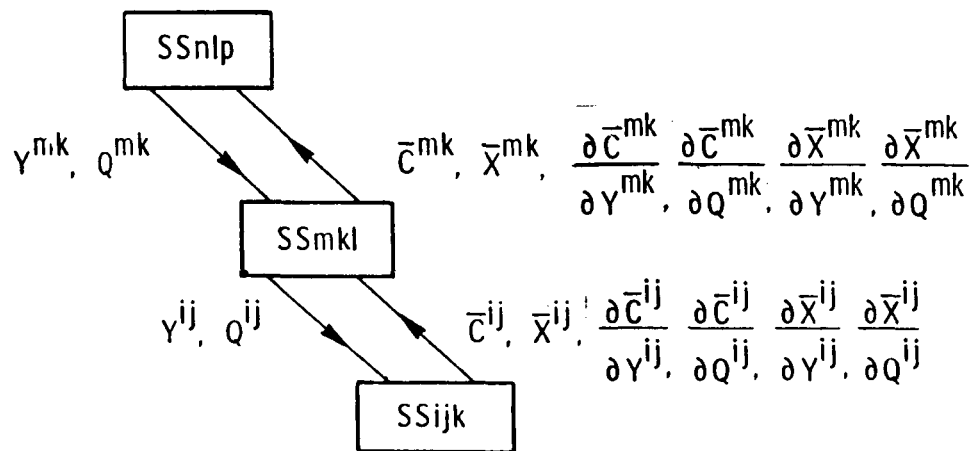


Figure 12. Flow of information.

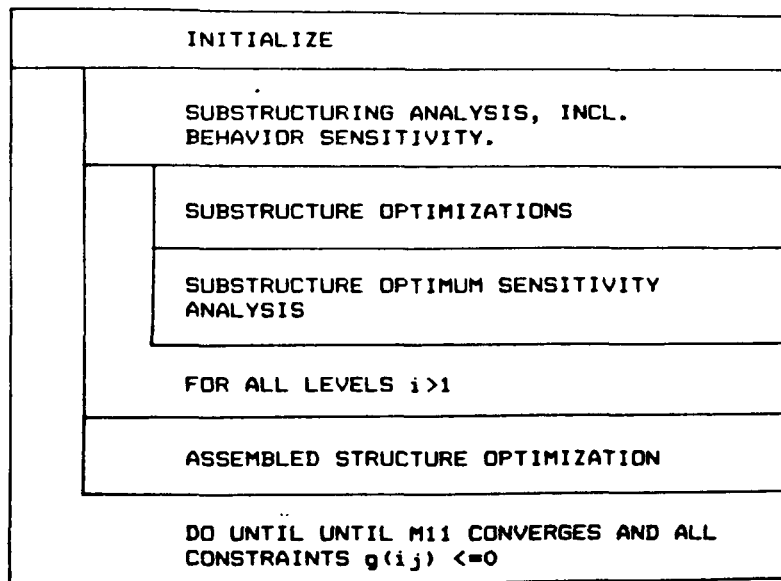


Figure 13. Multilevel optimization procedure flowchart.

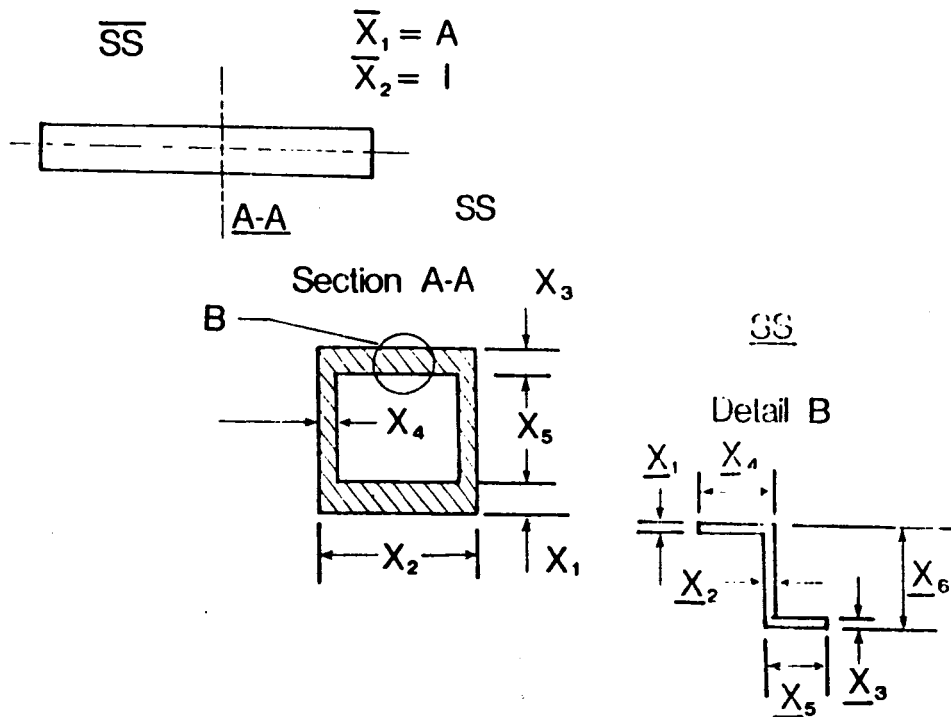
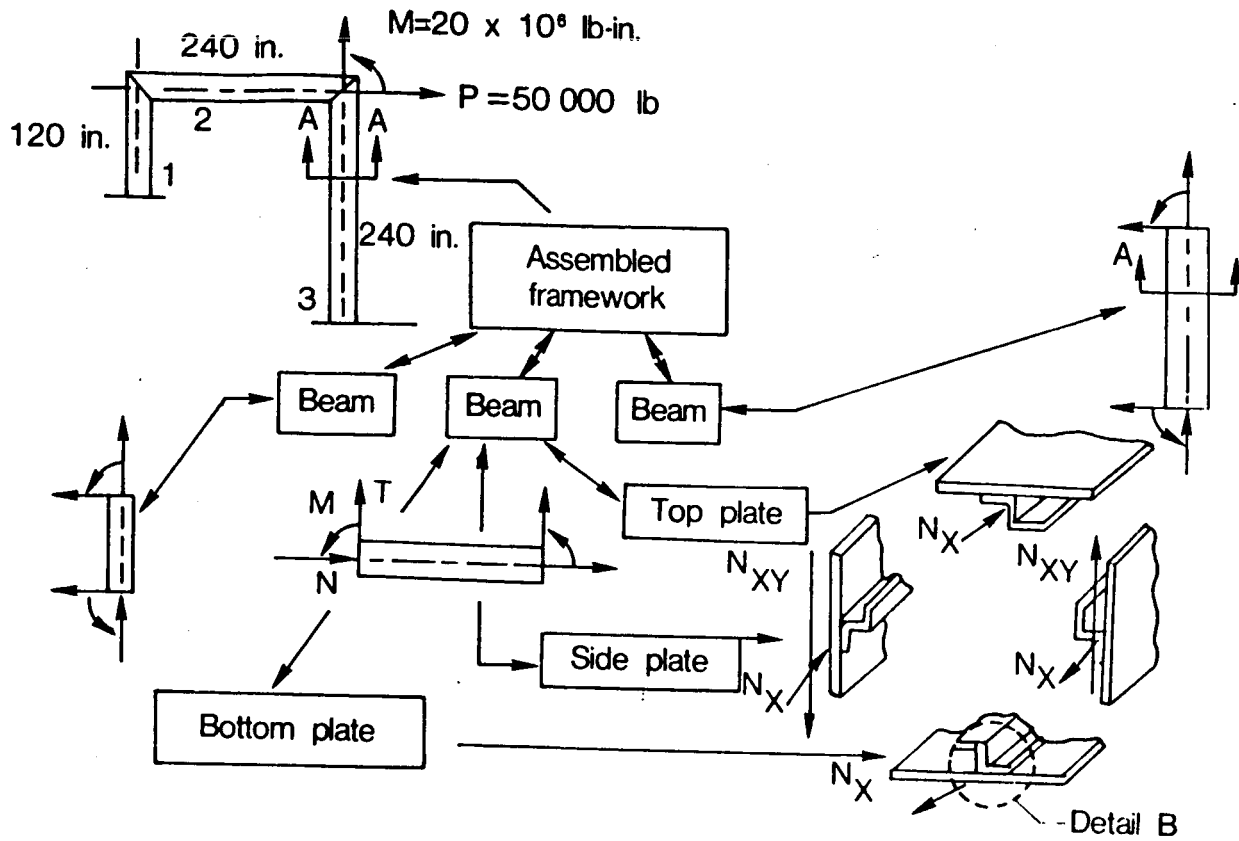


Figure 14. A portal framework.

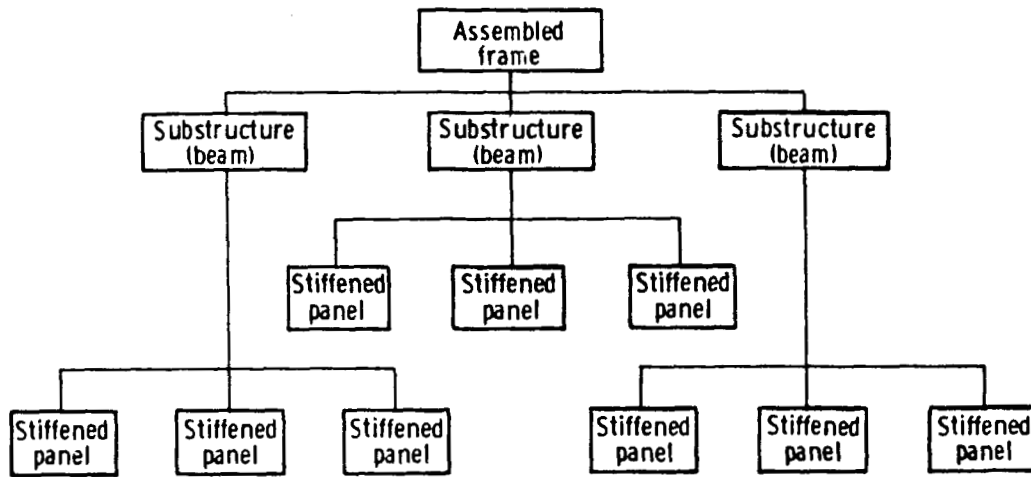
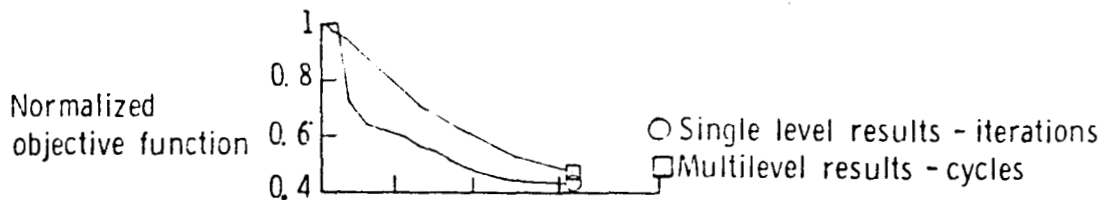


Figure 15. Hierarchical decomposition of the framework structure.



- ONE OF THE INDIVIDUAL CONSTRAINTS RECOGNIZED IN THE SINGLE LEVEL OPTIMIZATION.
- MULTILEVEL CUMULATIVE CONSTRAINT CONTAINING THE ABOVE INDIVIDUAL CONSTRAINT.
- ⊗ Single level displacement constraint
- ⊠ Multilevel displacement constraint

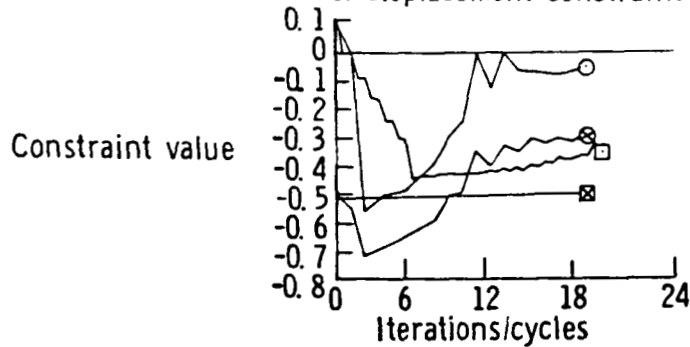


Figure 16. Representative results.

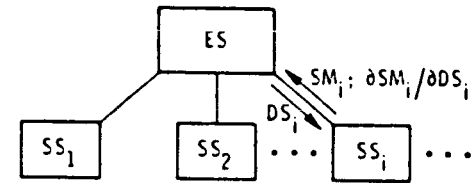
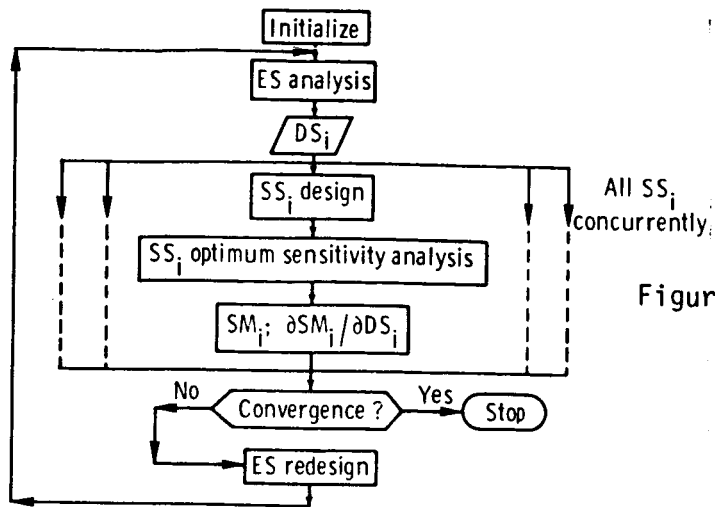


Figure 17. Typical two-level system.

Figure 18. Two-level system optimization procedure.

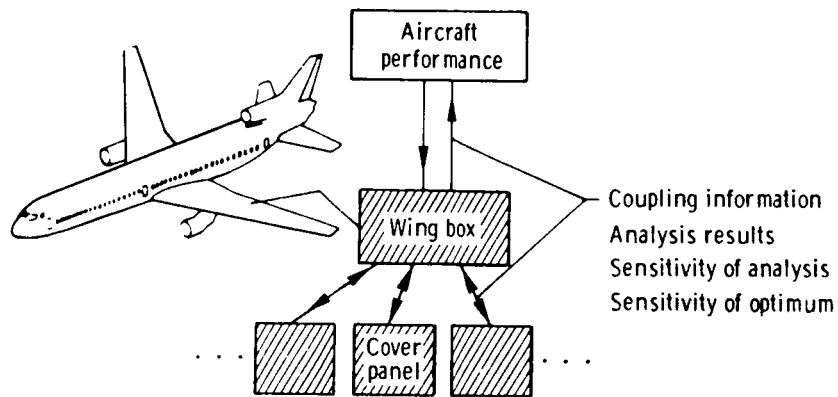


Figure 19. Aircraft and a schematic of its multilevel optimization.

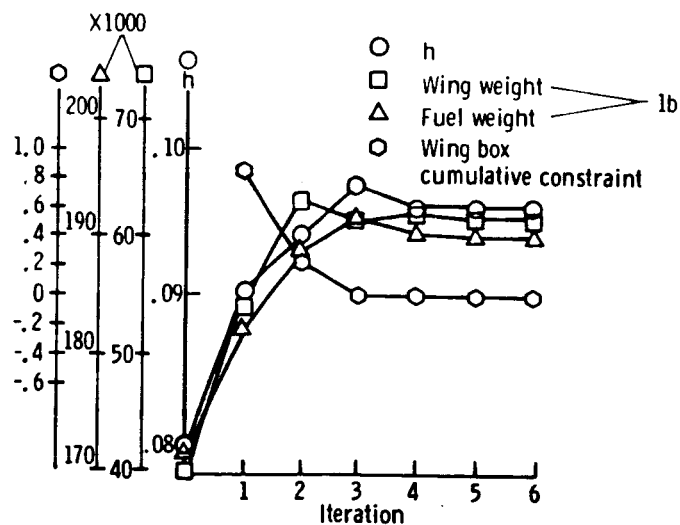


Figure 20. Histogram of an aircraft multilevel optimization.

Standard Bibliographic Page

1. Report No. NASA TM-89077		2. Government Accession No.		3. Recipient's Catalog No.	
4. Title and Subtitle Interdisciplinary and Multilevel Optimum Design				5. Report Date December 1986	
				6. Performing Organization Code 505-63-11	
7. Author(s) Jaroslaw Sobieszczanski-Sobieski and Raphael T. Haftka				8. Performing Organization Report No.	
				10. Work Unit No.	
9. Performing Organization Name and Address NASA Langley Research Center Hampton, VA 23665-5225				11. Contract or Grant No.	
				13. Type of Report and Period Covered Technical Memorandum	
12. Sponsoring Agency Name and Address National Aeronautics and Space Administration Washington, DC 20546-0001				14. Sponsoring Agency Code	
15. Supplementary Notes J. Sobieszczanski-Sobieski, Langley Research Center, Hampton, VA. Raphael T. Haftka, Virginia Polytechnic Institute and State University, Blacksburg, VA. Presented at the NATO Advanced Study Institute on Computer Aided Optimal Design, Troia, Portugal, July 1986.					
16. Abstract Interactions among engineering disciplines and subsystems in engineering system design are surveyed and specific instances of such interactions are described. Examination of the interactions demonstrates that a traditional design process in which the numerical values of major design variables are decided consecutively is likely to lead to a suboptimal design. Supporting numerical examples are a glider and a space antenna. Under an alternative approach introduced, the design and its sensitivity data from the subsystems and disciplines are generated concurrently and then made available to the system designer enabling him to modify the system design so as to improve its performance. Examples of a framework structure and an airliner wing illustrate that approach.					
17. Key Words (Suggested by Authors(s)) Design/optimization/multidisciplinary/ multilevel/integration/decomposition/ engineering system/subsystems/sensitivity				18. Distribution Statement Unclassified - Unlimited Subject Category 05	
19. Security Classif.(of this report) Unclassified		20. Security Classif.(of this page) Unclassified		21. No. of Pages 48	
				22. Price A03	

For sale by the National Technical Information Service, Springfield, Virginia 22161